PETROGENESIS OF EOCENE OCEANIC BASALTS FROM THE WEST PHILIPPINE BASIN AND OLIGOCENE ARC VOLCANICS FROM THE PALAU-KYUSHU RIDGE DRILLED AT 20°N, 135°E (WESTERN PACIFIC OCEAN)

Massimo D'Antonio*,✉, Ivan Savov, Piera Spadea***, Rosemary Hickey-Vargas°** and **John Lockwood°°**

* *Dipartimento di Scienze della Terra, Università Federico II, Napoli, Italy.*
** *Department of Terrestrial Magnetism, Carnegie Institution of Washington, U.S.A.*
*** *Dipartimento di Georisorse e Territorio, Università Udine, Italy.*
° *Department of Earth Sciences, Florida International University, Miami, FL., U.S.A.*
°° *Geohazards Consultants Inc., Private bag, Volcano, HI, U.S.A.*
✉ *Corresponding author, e-mail: masdanto@unina.it.*

Key-words: *Petrogenesis, mineral chemistry, geochemistry, radiogenic isotopes, Izu-Bonin-Mariana subduction factory, West Philippine Basin.*

ABSTRACT

The West Philippine Basin (WPB) is a back-arc basin that opened within the Philippine Sea Plate (PSP) between the current position of the Palau-Kyushu Ridge (PKR) and the margin of East Asia. Spreading occurred at the Central Basin Fault (CBF) mainly from 54 until 30 Ma. The PKR was active since ~48 to 35 Ma constituting a single volcanic arc with the Izu-Bonin-Mariana (IBM) Arc. At ~42 Ma ago spreading rate and direction changed from NE-SW to N-S, stopping at ~30 Ma. A late phase of spreading and volcanism took place between 30 and 26 Ma. ODP Leg 195 Site 1201 is located in the WPB, ~100 km west of the PKR, on 49 Ma crust formed by NE-SW spreading at the CBF. From ~35 to 30 Ma, pelagic sedimentation at Site 1201 was followed by turbidite sedimentation, fed mostly by arc-derived volcanic clasts. The geochemical and isotopic features of Site 1201 basement rocks, which represent Eocene WPB oceanic crust, compared with those of Site 1201 volcanics from the turbidite sequence, representing products of the early Mariana Arc (PKR), provide some insights into the early history of the IBM subduction factory. The WPB basement is made up of aphyric to porphyritic basalts with altered olivine, and preserved plagioclase, clinopyroxene and opaques. The PKR volcanics are porphyritic basalts and andesites with plagioclase, clino- and orthopyroxene, hornblende, alkali feldspar and opaques. Variable textures, and degree of alteration suggesting zeolite facies metamorphic grade, characterize both groups of rocks.

The mineralogical and geochemical characteristics of the investigated Site 1201 PKR volcanics highlight their calc-alkaline affinity. This feature is at variance with both other PKR rocks, having mostly boninitic and arc tholeiitic affinity, and WPB basement basalt, having tholeiitic affinity, with some characters transitional to arc-like, as expected for a back-arc basin. New Sr and Nd isotope data, coupled with published Sr, Nd, Pb and Hf isotope data (Savov et al., 2006), highlight the Indian Ocean MORB-like character of Site 1201 basement basalts. This suggests that WPB volcanism tapped an upper mantle domain distinct from that underlying the Pacific Plate. The isotopic features of Site 1201 PKR volcanics are more enriched relative to those of basement basalts reflecting higher amounts of subduction-derived component(s) in the source of arc magmas. Th-Nb relationships and isotope geochemistry of the WPB basement and overlaying arc volcanics suggest addition of subducted sediment mostly as siliceous melts, to the mantle source of the arc volcanics. In that respect, Site 1201 PKR volcanics resemble calc-alkaline volcanics of the currently active Mariana Arc. In addition, the calc-alkaline affinity, unradiogenic neodymium, and inferred Middle Oligocene age of PKR volcanics, suggest they might represent an evolved stage of arc volcanism at Palau-Kyushu Ridge, perhaps shortly before the end of its activity.

INTRODUCTION

During Ocean Drilling Program (ODP) Leg 195 in Western Pacific Ocean (March-May 2001), a 453 m thick sequence of turbidites containing volcanic clasts, overlying 94 m of basaltic pillows and hyaloclastites, was recovered at Site 1201, Hole D (Salisbury, Shinohara, Richter et al., 2002; Salisbury et al., 2006). Geological, volcanological and petrological interpretation of the entire volcanic sequence cored at Site 1201 and several adjacent Deep Sea Drilling Project (DSDP) Sites revealed that turbidites contain volcanic clasts derived from a paleo-volcanic island arc, whereas the basement basalts erupted in a back-arc basin setting (Salisbury, Shinohara, Richter, et al., 2002; Savov et al., 2006). These findings provide a unique opportunity for investigating the nature and relationships between magmas erupting at the volcanic front of arcs versus those feeding back-arc spreading centers. The investigated arc-basin system is part of the Izu-Bonin-Mariana (IBM) subduction factory located in the West Philippine Basin (Fig. 1), characterized by complex geodynamic setting and evolution through time (see Stern et al., 2004, and Pearce et al., 2005, for a review).

The West Philippine Basin (WPB) is located within the Philippine Sea Plate (PSP) between the Palau-Kyushu Ridge (PKR) and the eastern margin of Asia (Fig. 1). During ODP Leg 195 in the WPB, Site 1201, Hole D was drilled in 5711 m of water, about 100 km west of the PKR and 450 km north of the Central Basin Fault (CBF). At present, this submerged ridge represents an inactive spreading center, which generated the oceanic crust building the WPB basement. The main spreading phase at CBF occurred from ~55 to 30 Ma (Hilde and Lee, 1984; Hall et al., 1995; Fujioka et al, 1999; Deschamps and Lallemand, 2002; Deschamps et al., 2002). Based on interpretations of the magnetic lineations (Hilde and Lee, 1984), Site 1201 lies on 49 Ma crust (Chron 21, Fig. 1) formed by NE-SW spreading at the CBF. The PKR and the IBM arc constituted a single volcanic front, active between ~48 and 35 Ma (Arculus et al., 1995; Cosca et al., 1998; Stern et al., 2004). At ~42 Ma the spreading rate and direction changed to N-S (Hussong and Uyeda, 1981), stopping at ~30 Ma (Deschamps and Lallemand, 2002) as

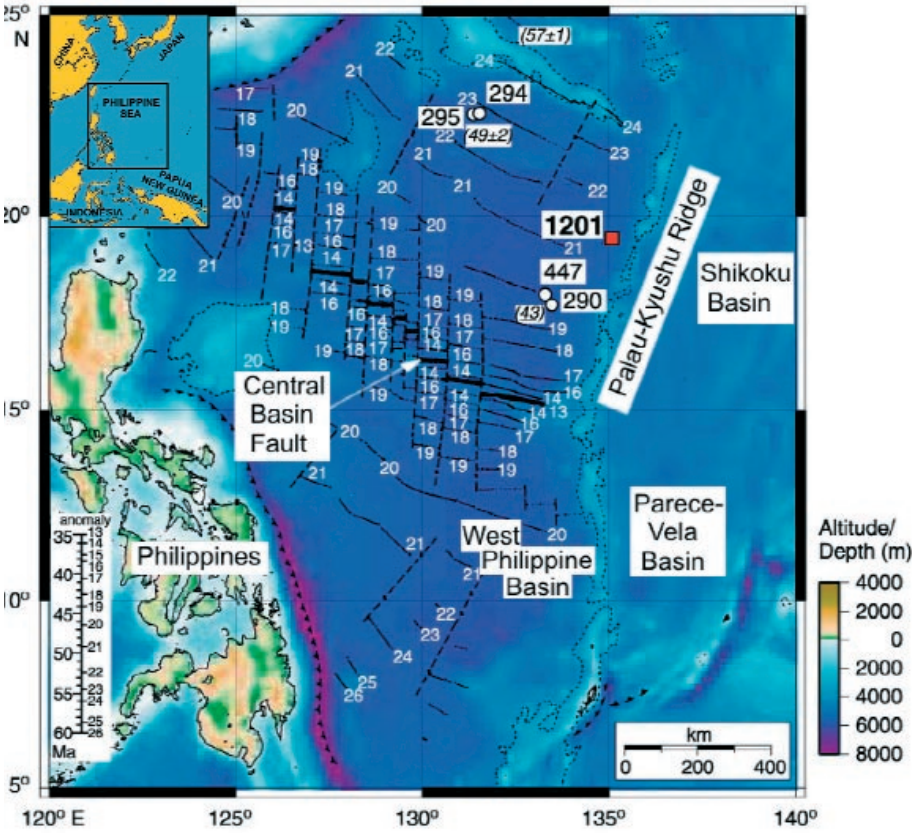

Fig. 1 - Sketch map showing the main basins and ridges in the Western Pacific Ocean (modified after Salisbury, Shinohara, Richter, et al., 2002). Large numbers indicate either DSDP or ODP drilling sites (red square indicates the location of ODP Site 1201); smaller numbers in parentheses are ages inferred from magnetic lineations, white small numbers indicate Chrons (Hilde and Lee, 1984). The inset shows the location of the study area (boxed) in relation to Japan, China, Indonesia and Papua-New Guinea.

volcanism ceased at the PKR (Hilde and Lee, 1984). However, late spreading and/or volcanism may have continued between 30 and 26 Ma (Scott and Kroenke, 1983; Cosca et al., 1998; Deschamps et al., 1999; 2002; Fujioka et al., 1999; Okino et al., 1999; Deschamps and Lallemand, 2002) in response to opening of the Parece Vela and Shikoku back-arc basins to the east (Fig. 1). These basins formed as a consequence of renewed subduction and hinge roll-back of the Pacific Plate along the eastern Philippine Sea Plate margin. Roll-back of the Pacific Plate triggered E-W intra-arc rifting (Hall, 2002; Deschamps et al., 2002), leaving an inactive segment to the west (the Palau-Kyushu Ridge remnant arc) and shifting arc volcanism to its current location at the Izu-Bonin-Mariana arc front. In the Late Eocene to Middle Oligocene (from ~35 to 30 Ma), pelagic sedimentation at Site 1201 was followed by flysch sedimentation, fed by island arc-derived volcanic clasts mixed with reef detritus (Salisbury, Shinohara, Richter, et al., 2002).

In this paper we present new mineral chemistry, and bulk-rock geochemical and Sr-Nd-isotopic data for Site 1201 calc-alkaline volcanic clasts and polymict tuffs derived from the Palau-Kyushu Ridge (proto IBM arc). These data are integrated with those published for three well-studied large volcanic clasts from the PKR and for a suite of well-studied basement basalts from Site 1201 (D'Antonio and Kristensen, 2005a; Savov et al., 2006) representing old WPB oceanic crust. The comparison will provide important insights into the early history of the IBM subduction factory. In chaotic terranes like melanges or variegated formations, studying ancient volcaniclastic sequences in tectonic or lithostratigraphic proximity to supra-subduction zone ophiolites, may provide extremely valuable information about the temporal evolution of entire supra-subduction basins including the forearc, arc and back-arc regions. Therefore, our results, combined with existing data for the same region (currently with active volcanism) provide a much needed baseline for such comparisons.

PETROGRAPHY

The turbidite sequence recovered at Site 1201 includes 24 cores (1R to 24R) made up of PKR volcanic clasts (mainly lava fragments mm- to dm-sized), and abundant single crystals (up to 2-3 mm in size), variably dispersed in a clay-rich matrix, containing rare fossil shell fragments. Considering the large variety of lithological types, the recovered volcanogenic sequence can be considered as made up of polymict tuffs (Fig. 2A). The clasts consist of highly vesicular basic to intermediate calc-alkaline volcanic rocks (Fig. 2B-C). The textures are generally porphyritic and/or glomeroporphyritic (15-30% phenocrysts), with groundmass exhibiting various textural types including intergranular, intersertal, felty and pilotaxitic. The phenocrysts are strongly altered olivine (in basic rocks), plagioclase (partially altered to secondary alkali-feldspar, zeolites and calcite), generally fresh clinopyroxene, orthopyroxene, rare hornblende (in intermediate rocks), and diffuse opaque oxides, likely Ti-magnetite. The clast groundmass contains variable amounts of recrystallized or zeolitized, black to brown glass. Single crystals in the matrix are mostly plagioclase, variably altered to secondary alkali-feldspar, zeolites and calcite, and minor fresh pyroxene. The silt- to sand-sized matrix is a mixture of clay minerals, iron oxyhydroxides ("iddingsite") and calcite. Considering this secondary mineral association, it can be inferred that Site 1201 volcanic clasts in turbidites suffered low temperature alteration in a generally oxidizing environment.

The Site 1201 basement basalts (WPB) occur as mostly pillows and minor massive lavas (Fig. 2D-E-F). The rocks

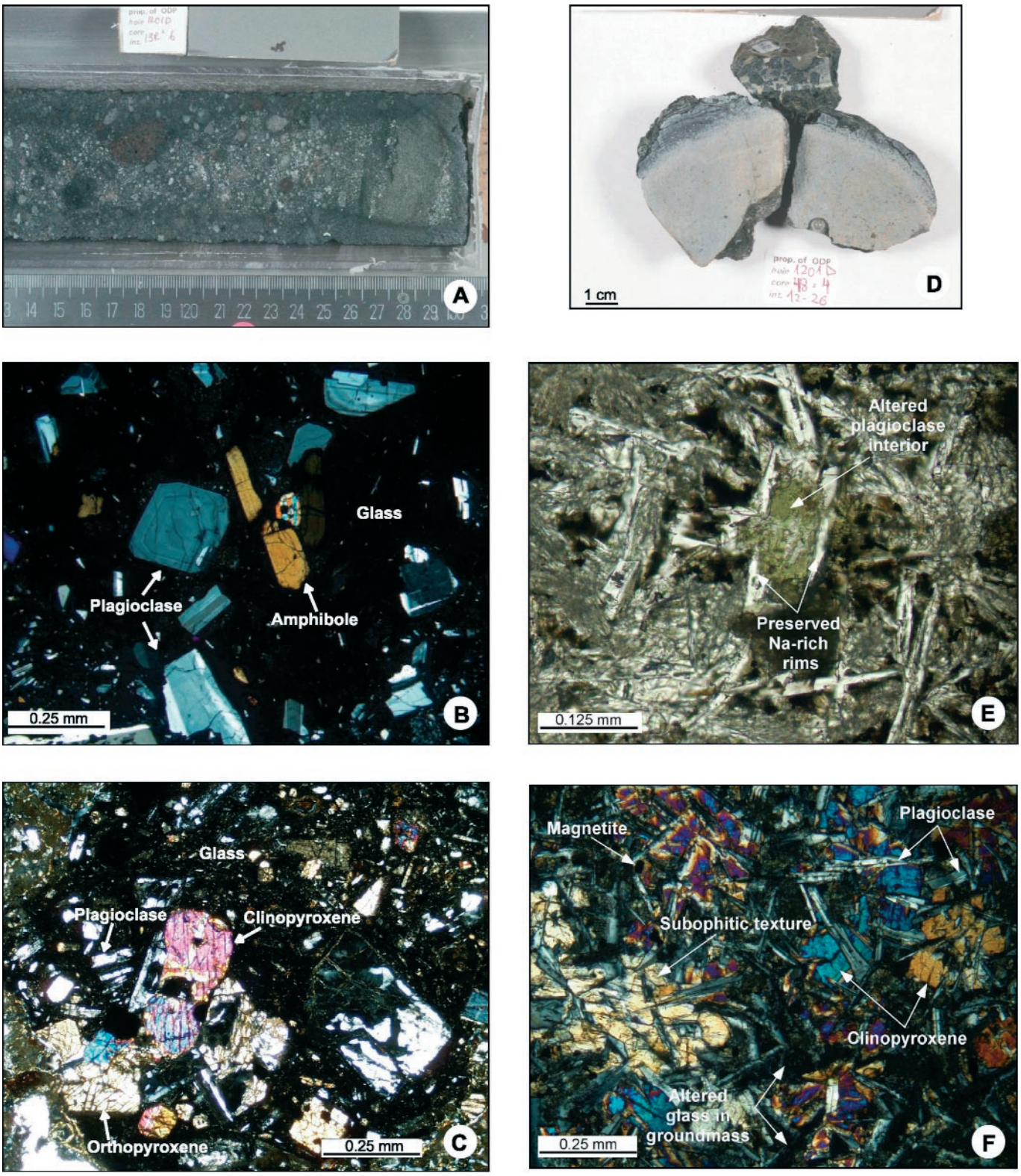

Fig. 2 - Typical macro- and micro-petrographic features of Site 1201 volcanic rocks. A) Photograph of a polymict tuff from the turbidite sequence (interval 195-1201D-13R-6, 113-130 cm), consisting of several volcanic clasts included in a clay-rich matrix (Salisbury, Shinohara, Richter, et al., 2002); B) photomicrograph showing typical mineral paragenesis and texture of a glass-rich volcanic clast (sample 195-1201D-2R-2, 74-77 cm; cross-polarized light); C) photomicrograph showing typical mineral paragenesis and texture of a highly porphyritic volcanic clast (sample 195-1201D-18R-3, 122-125 cm; cross-polarized light); D) photograph of fragments of a pillow basalt and hyaloclastite from the basement sequence (interval 195-1201D-48R-4, 12-26 cm; Salisbury, Shinohara, Richter, et al., 2002); E) photomicrograph showing typical texture of a glassy aphyric basement basalt (sample 195-1201D-48R-2, 74-76 cm; plane-polarized light; Salisbury, Shinohara, Richter, et al., 2002); F) photomicrograph showing typical mineral paragenesis and texture of a moderately porphyritic basement basalt (sample 195-1201D-55R-1, 103-106 cm; cross-polarized light; Salisbury, Shinohara, Richter, et al., 2002).

are aphyric to porphyritic (up to ~7 % phenocrysts), with variable degree of alteration (LOI = 0.77-11.85 wt.%; Salisbury, Shinohara, Richter, et al., 2002). The primary minerals consist of: plagioclase, ranging in composition from labradorite through bytownite to andesine; olivine (presumably magnesian, now completely replaced by secondary minerals); chromian-magnesian-diopside; Ti-magnetite (partially maghemitized) and chromian spinel. Mineral paragenesis, composition of relict primary minerals and geothermobarometric estimates suggest a rather primitive composition for the parent magmas (D'Antonio and Kristensen, 2005a). Glass-rich basalts exhibit spherulitic, hyalopilitic and branching textures (Fig. 2E). More crystallized basalts show felty, intersertal, intergranular and subophitic textures (Fig. 2F). The volcanic glass is devitrified to clay minerals and zeolites. Skeletal, swallow-tailed plagioclase crystals are commonly replaced by calcite, alkali feldspar and Ca-Na-zeolites. Euhedral crystals of former olivine are completely replaced by clay minerals, iron oxyhydroxides ("iddingsite") and calcite. Clay minerals are K-Fe-Mg-rich (mostly glauconite, minor Al-saponite and Fe-beidellite), whereas zeolites are Ca-Na-rich (natrolite group zeolites and analcite). The secondary minerals paragenesis suggests zeolite facies metamorphic grade, likely occurred under mostly oxidizing conditions at temperatures not exceeding 100-150°C (D'Antonio and Kristensen, 2005b).

MINERAL CHEMISTRY

Selected electron microprobe analyses for preserved minerals (pyroxene and plagioclase) occurring in Site 1201 volcanic clasts and as single crystals within the matrix enclosing the clasts, are presented in Tables 1, 2 and 3. These data are plotted on conventional mineralogical diagrams in Figs. 3 (Diopside-Hedenbergite-Enstatite-Ferrosilite) and 4 (Albite-Anorthite-Orthoclase) together with available data for Site 1201 basement basalts (from D'Antonio and Kristensen, 2005a). Literature data for other samples from the Palau-Kyushu Ridge drilled during DSDP Leg 59 (Ishii, 1980; Scott, 1980) are also shown for comparison.

Pyroxenes

Chemical analyses of pyroxene are plotted on the quadrilateral classification diagram Di-Hd-En-Fs (Fig. 3). This diagram reveals that both clinopyroxene and orthopyroxene are present in the volcanic clasts (Fig. 3A) and also within the single crystals population of the matrix (Fig. 3B). According to their Wo, En and Fs contents, the clinopyroxene crystals plot in the field of magnesium-rich augite, and are often aluminian, and sometimes also ferrian and chromian (Table 1). The orthopyroxene is ferroan enstatite, sometimes aluminian and/or ferrian (Table 2; classification and nomenclature according to Rock, 1990 and Yavuz, 2001). The augites have Mg# [= atomic 100 x $Mg^{2+}/(Mg^{2+}+Fe^{2+}+Mn^{2+})$] ranging between 83.4 and 62.4. More primitive crystals (Mg# reaching up to 83.4) also have relatively high Cr_2O_3 contents (up to 0.35 wt%). Moreover, clinopyroxene crystals display a trend of decreasing En and Wo with increasing Fs on the quadrilateral classification diagram (Fig. 3). This trend is typical of clinopyroxenes from calc-alkaline basalts and andesites (e.g., Ewart, 1982); however, it is not exclusive of calc-alkaline series, since it has also been described for clinopyroxenes from mid-ocean ridge tholeiites (e.g., Hodges and Papike, 1977; Dungan et al., 1978; Mevel et al., 1978; Wood et al., 1979). The enstatites have a relatively narrow range of Mg# (74.1-61.3), only partially overlapping that of augites, and show a trend of enrichment in Fs content which mirrors that of augites. The coupled variation of high-Ca and low-Ca pyroxenes is typical of calc-alkaline basalts and andesites. Literature data for pyroxenes from the Palau-Kyushu Ridge (Ishii, 1980; Scott, 1980; Hawkins and Castillo, 1998) display overall comparable variations; however, these studies also report some extreme Fe-augite and pigeonite compositions that are missing in Site 1201 volcanic clasts and crystal population within the matrix (Fig. 3C).

In Site 1201 basement basalts only clinopyroxene is present. It classifies as chromian-magnesian-augite, with a total range of Mg# between 88.0 and 71.3 (D'Antonio and Kristensen, 2005a) denoting a more primitive character of the magmas in comparison to the volcanic clasts from the PKR arc.

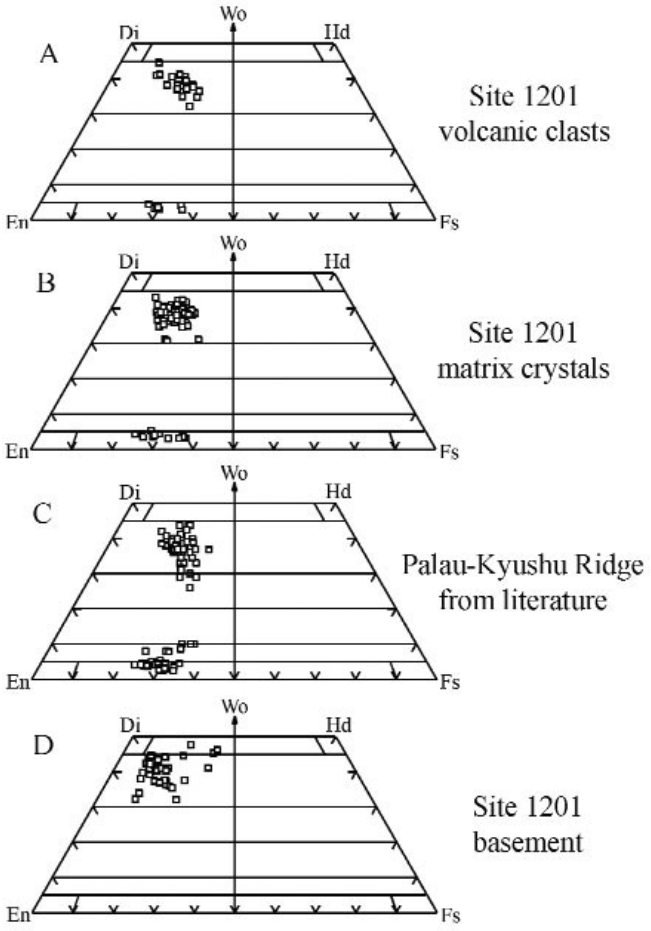

Fig. 3 - Classification diagram Di-Hd-En-Fs for pyroxenes (Rock, 1990), showing the chemical variability of pyroxenes of A) Site 1201 volcanic clasts (this work), B) Site 1201 matrix single crystals (this work), C) Palau-Kyushu Ridge (data from DSDP Leg 59, Sites 448, 448A and 451; Ishii, 1980; Scott, 1980) and D) Site 1201 basement basalts (D'Antonio and Kristensen, 2005a). Di- diopside; Hd- hedenbergite; En- enstatite; Fs- ferrosilite; Wo- wollastonite.

Table 1 - Representative electron microprobe analyses of clinopyroxene from Site 1201 volcanic clasts and matrix crystals

Sample	2R-1, 135-137	10R-4, 63-66	10R-4, 63-66	11R-1, 83-85	15R-2, 125-127	18R-3, 122-125	1R-1, 119-121	3R-3, 27-29	11R-1, 83-85	13R-6, 116-119	15R-2, 72-75	18R-3, 122-125
Type	volc. clast	volc. clast	volc. clast	volc. clast	volc. clast	volc. clast	matrix xtl	matrix xtl	matrix xtl	matrix xtl	matrix xtl	matrix xtl
Analysis No.	7a	2a	3a	5	7a3	5	1	4	7a	3	7a	1a
Classification (Rock, 1990)	aluminian chromian Mg-rich augite	aluminian Mg-rich augite	Mg-rich augite	aluminian Mg-rich augite	aluminian Mg-rich augite	aluminian Mg-rich augite	aluminian Mg-rich augite	Mg-rich augite	aluminian Mg-rich augite	aluminian Mg-rich augite	aluminian ferrian Mg-rich augite	aluminian Mg-rich augite
SiO_2	51.95	51.10	51.46	52.10	50.13	51.17	52.09	50.57	50.99	51.41	50.41	51.08
TiO_2	0.33	0.45	0.47	0.46	0.73	0.42	0.34	0.56	0.55	0.48	0.21	0.39
Al_2O_3	2.72	2.35	1.80	2.74	2.44	2.78	2.54	2.08	2.58	3.16	2.46	2.81
FeOtot	6.92	10.84	11.36	9.05	13.10	11.54	9.06	14.26	13.04	9.50	8.36	12.34
MnO	0.15	0.25	0.34	0.28	0.22	0.28	0.23	0.54	0.36	0.22	0.18	0.27
MgO	16.44	15.38	14.65	16.51	14.27	14.60	15.74	13.77	13.89	14.91	18.34	14.63
CaO	19.83	18.80	19.14	18.65	18.24	19.17	19.15	17.44	18.55	19.67	18.48	18.50
Na_2O	0.23	0.25	0.33	0.28	0.23	0.28	0.28	0.28	0.38	0.24	0.15	0.25
Cr_2O_3	0.35	0.09	b.d.l.	0.21	b.d.l.	0.27	0.14	0.05	b.d.l.	b.d.l.	0.11	b.d.l.
Sum	98.93	99.51	99.55	100.27	99.36	100.51	99.56	99.56	100.34	99.58	98.70	100.26
Fe_2O_3	0.85	2.59	2.10	1.59	2.88	2.66	0.78	2.33	2.47	0.81	5.80	2.38
FeO	6.16	8.50	9.47	7.62	10.51	9.15	8.35	12.16	10.82	8.78	3.14	10.21
Sum	99.01	99.77	99.76	100.42	99.65	100.78	99.64	99.80	100.59	99.67	99.28	100.50
Si	1.928	1.908	1.929	1.916	1.893	1.900	1.934	1.915	1.907	1.915	1.865	1.903
Al^{IV}	0.072	0.092	0.071	0.084	0.107	0.100	0.066	0.085	0.093	0.085	0.107	0.097
Al^{VI}	0.047	0.012	0.009	0.035	0.001	0.022	0.045	0.008	0.020	0.053	0.000	0.026
Ti	0.009	0.013	0.013	0.013	0.021	0.012	0.009	0.016	0.015	0.013	0.006	0.011
Cr	0.010	0.003	0.000	0.006	0.000	0.008	0.004	0.002	0.000	0.000	0.003	0.000
Fe^{3+}	0.024	0.073	0.059	0.044	0.082	0.074	0.022	0.066	0.070	0.023	0.162	0.067
Fe^{2+}	0.191	0.266	0.297	0.234	0.332	0.284	0.259	0.385	0.338	0.273	0.097	0.318
Mn	0.005	0.008	0.011	0.009	0.007	0.009	0.007	0.017	0.011	0.007	0.006	0.008
Mg	0.909	0.856	0.819	0.905	0.803	0.808	0.871	0.778	0.775	0.828	1.011	0.813
Ca	0.788	0.752	0.769	0.735	0.738	0.763	0.762	0.708	0.743	0.785	0.733	0.739
Na	0.016	0.018	0.024	0.020	0.017	0.020	0.020	0.021	0.027	0.017	0.010	0.018
Sum	4.000	4.000	4.000	4.000	4.000	4.000	4.000	4.000	4.000	4.000	4.000	4.000
Ca at.%	41.12	38.49	39.34	38.14	37.62	39.35	39.65	36.22	38.36	40.97	36.48	37.99
Mg at.%	47.43	43.80	41.88	46.97	40.93	41.71	45.34	39.79	39.99	43.22	50.35	41.79
Fe* at.%	11.45	17.71	18.77	14.89	21.44	18.94	15.01	23.99	21.65	15.80	13.17	20.21
Mg#	80.55	71.20	69.05	75.92	65.62	68.77	75.12	62.39	64.87	73.22	79.27	67.40

All sample labels are preceded by 195-1201D. Formulae calculated on the basis of 6 oxygens (software PYROX; Yavuz, 2001). Mg# = $100*Mg^{2+}/(Mg^{2+}+Fe^{2+}+Mn^{2+})$. Fe* = $Fe^{3+}+Fe^{2+}+Mn^{2+}$. b.d.l. = below detection limit. Major oxides are reported as wt%, cations as atoms per formula unit. At.% = atomic percentage. Data were determined by electron microprobe analysis techniques using a JEOL JXA-8900R SuperProbe, equipped with 5 wavelength dispersive spectrometers, at the Florida Center for Analytical Electron Microscopy, Florida International University, Miami, USA. Running conditions were: 15 kV accelerating voltage, 20nA current, 1 µ spot size, 10s counting times for each element, 5s for background. Diopside and albite were used as standards.

Table 2 - Representative electron microprobe analyses of orthopyroxene from Site 1201 volcanic clasts and matrix crystals

Sample	1R-1, 119-121	2R-1, 135-137	10R-4, 63-66	10R-4, 63-66	13R-6, 116-119	2R-2, 8-10	10R-4, 63-66	15R-2, 72-75	15R-2, 72-75	18R-3, 122-125	18R-3, 122-125	24R-4, 70-72
Type	volc. clast	volc. clast	volc. clast	volc. clast	volc. clast	matrix xtl	matrix xtl	matrix xtl	matrix xtl	matrix xtl	matrix xtl	matrix xtl
Analysis No.	4-2	5a	2	6	4	0	4	4a2	4d	3b	4	3b
Classification (Rock, 1990)	ferroan enstatite	ferroan enstatite	ferroan enstatite	ferroan enstatite	ferroan enstatite	aluminian ferrian ferroan enstatite	ferroan enstatite	ferroan enstatite	ferrian ferroan enstatite	ferrian ferroan enstatite	ferroan enstatite	aluminian ferroan enstatite
SiO_2	52.80	53.04	52.22	52.35	51.73	51.47	51.60	51.79	50.58	51.92	52.46	52.81
TiO_2	0.24	0.17	0.30	0.26	0.25	0.19	0.26	0.26	0.28	0.23	0.21	0.14
Al_2O_3	1.57	0.96	1.39	1.44	1.03	3.63	1.73	0.97	0.97	1.85	2.23	2.41
FeOtot	19.07	19.11	22.32	18.74	23.50	16.26	22.18	23.03	23.41	18.51	19.48	16.84
MnO	0.47	0.61	0.65	0.43	0.75	0.38	0.56	0.82	0.84	0.39	0.42	0.32
MgO	24.60	23.77	21.69	23.63	21.59	26.77	21.18	21.60	22.35	24.55	23.89	25.68
CaO	1.96	1.47	1.99	2.16	1.56	1.74	1.75	1.67	1.45	1.99	1.94	1.70
Na_2O	0.01	0.02	0.04	0.09	0.02	0.06	0.04	0.03	0.01	0.11	0.01	0.01
Cr_2O_3	0.07	0.06	b.d.l.	0.08	b.d.l.	0.04	0.05	b.d.l.	b.d.l.	b.d.l.	0.17	0.05
Sum	100.78	99.20	100.60	99.18	100.43	100.54	99.35	100.16	99.89	99.56	100.79	99.95
Fe_2O_3	2.94	0.61	1.82	1.94	3.05	5.75	1.14	2.74	5.85	3.83	2.50	2.13
FeO	16.42	18.56	20.69	16.99	20.75	11.08	21.15	20.56	18.15	15.07	17.23	14.92
Sum	101.08	99.26	100.78	99.37	100.73	101.11	99.46	100.43	100.48	99.94	101.04	100.16
Si	1.920	1.966	1.937	1.938	1.928	1.843	1.940	1.934	1.889	1.905	1.912	1.916
Al^{IV}	0.067	0.034	0.061	0.062	0.045	0.153	0.060	0.043	0.043	0.080	0.088	0.084
Al^{VI}	0.000	0.008	0.000	0.000	0.000	0.000	0.016	0.000	0.000	0.000	0.008	0.019
Ti	0.006	0.005	0.008	0.007	0.007	0.005	0.007	0.007	0.008	0.006	0.006	0.004
Cr	0.002	0.002	0.000	0.002	0.000	0.001	0.002	0.000	0.000	0.000	0.005	0.001
Fe^{3+}	0.080	0.017	0.051	0.054	0.086	0.155	0.032	0.077	0.164	0.106	0.069	0.058
Fe^{2+}	0.499	0.575	0.642	0.526	0.647	0.332	0.665	0.642	0.567	0.462	0.525	0.453
Mn	0.014	0.019	0.020	0.014	0.024	0.012	0.018	0.026	0.027	0.012	0.013	0.010
Mg	1.333	1.314	1.199	1.304	1.200	1.429	1.187	1.203	1.244	1.342	1.298	1.389
Ca	0.076	0.058	0.079	0.086	0.062	0.067	0.070	0.067	0.058	0.078	0.076	0.066
Na	0.000	0.001	0.003	0.007	0.001	0.004	0.003	0.002	0.001	0.008	0.001	0.000
Sum	4.000	4.000	4.000	4.000	4.000	4.000	4.000	4.000	4.000	4.000	4.000	4.000
Ca at.%	3.81	2.95	3.97	4.33	3.09	3.34	3.57	3.31	2.82	3.91	3.83	3.35
Mg at.%	66.54	66.22	60.24	65.75	59.45	71.66	60.17	59.70	60.41	67.09	65.54	70.30
Fe* at.%	29.65	30.83	35.79	29.93	37.47	25.00	36.26	36.98	36.78	29.00	30.63	26.35
Mg#	69.17	68.23	62.73	68.72	61.34	74.14	62.40	61.75	62.16	69.82	68.15	72.73

All sample labels are preceded by 195-1201D. Formulae calculated on the basis of 6 oxygens (software PYROX; Yavuz, 2001). Mg# = $100*Mg^{2+}/(Mg^{2+}+Fe^{2+}+Mn^{2+})$. Fe* = $Fe^{3+}+Fe^{2+}+Mn^{2+}$. b.d.l. = below detection limit. Major oxides are reported as wt%, cations as atoms per formula unit. At.% = atomic percentage. For analytical techniques see footnote to Table 1.

Table 3 - Representative electron microprobe analyses of plagioclase from Site 1201 volcanic clasts and matrix crystals

Sample	1R-1, 119-121	1R-1, 119-121	10R-4, 63-66	11R-1, 83-85	11R-1, 83-85	15R-2, 125-127	1R-1, 119-121	10R-4, 63-66	11R-1, 83-85	11R-1, 83-85	11R-1, 83-85	11R-1, 83-85
Type	volc. clast	volc. clast	volc. clast	volc. clast	volc. clast	volc. clast	matrix xtl	matrix xtl	matrix xtl	matrix xtl	matrix xtl	matrix xtl
Analysis No.	2c	4-3	2	3	3b	7c	1a	7a	4a	2c	2e	2f
Classification	bytownite	bytownite	labradorite	labradorite	bytownite	bytownite	bytownite	labradorite	labradorite	labradorite	bytownite	labradorite
SiO_2	51.62	47.58	52.27	55.00	50.02	47.95	47.54	51.45	51.71	51.65	50.41	51.00
TiO_2	0.06	0.02	0.05	0.03	0.00	0.05	0.01	0.04	0.05	0.03	0.02	0.04
Al_2O_3	30.44	32.44	28.70	28.39	31.23	31.72	32.78	29.82	29.55	29.63	30.12	30.01
Fe_2O_3 #	0.99	0.79	1.12	0.48	0.80	0.84	0.83	0.93	0.69	0.88	0.78	0.98
MgO	0.21	0.09	0.15	0.05	0.16	0.16	0.17	0.16	0.22	0.16	0.13	0.12
CaO	13.56	16.14	12.55	10.79	14.94	15.23	15.08	13.25	13.37	13.65	13.88	13.65
Na_2O	2.67	1.93	3.49	4.35	2.65	2.46	2.07	3.21	3.41	3.47	3.16	3.34
K_2O	0.08	0.07	0.19	0.14	0.10	0.07	0.07	0.12	0.14	0.11	0.13	0.15
Sum	99.64	99.05	98.52	99.23	99.88	98.48	98.54	98.97	99.14	99.58	98.64	99.29
Si	9.399	8.814	9.624	9.959	9.145	8.922	8.822	9.444	9.480	9.444	9.313	9.360
Ti	0.008	0.003	0.006	0.003	0.000	0.007	0.001	0.005	0.007	0.004	0.003	0.006
Al	6.532	7.081	6.229	6.059	6.729	6.956	7.169	6.452	6.384	6.384	6.559	6.492
Fe^{3+}	0.136	0.110	0.156	0.066	0.110	0.117	0.116	0.128	0.095	0.122	0.109	0.135
Mg	0.058	0.024	0.042	0.014	0.042	0.043	0.046	0.043	0.061	0.043	0.036	0.034
Ca	2.646	3.202	2.476	2.093	2.928	3.036	2.999	2.605	2.627	2.675	2.748	2.684
Na	0.944	0.693	1.244	1.529	0.938	0.889	0.746	1.141	1.212	1.229	1.132	1.188
K	0.019	0.016	0.044	0.033	0.022	0.017	0.016	0.028	0.033	0.027	0.031	0.036
Sum	19.740	19.943	19.822	19.756	19.915	19.987	19.915	19.845	19.897	19.927	19.932	19.933
An mol.%	73.33	81.87	65.78	57.27	75.30	77.02	79.74	69.04	67.85	68.06	70.26	68.69
Ab mol.%	26.15	17.72	33.05	41.83	24.13	22.54	19.83	30.23	31.30	31.27	28.95	30.39
Or mol.%	0.52	0.40	1.17	0.90	0.57	0.44	0.43	0.73	0.85	0.68	0.78	0.92

All sample labels are preceded by 195-1201D. Formulae calculated on the basis of 32 oxygens. #: all Fe as Fe_2O_3. b.d.l. = below detection limit. Major oxides are reported as wt%, cations as atoms per formula unit. Mol.% = molar percentage. For analytical techniques see footnote to Table 1.

Plagioclase

In the Site 1201 volcanoclastic sequence primary plagioclase occurs both in individual clasts and as single crystals within the turbidite matrix. The plagioclase chemical data are plotted separately on the ternary Ab-An-Or classification diagram (Fig. 4A, B). The anorthite content of plagioclase crystals from the volcanic clasts ranges from An_{95} to An_{53}, whereas single crystals in the matrix display a more restricted range, between An_{85} and An_{54} (Table 3). The Or content is generally lower than 1 wt%, and may reach 1.3 wt%. Overall, the majority of plagioclase crystals fall in the bytownite and labradorite fields (Fig. 4A, B), within the large variability range (An_{93} to An_{27}) displayed by Palau-Kyushu Ridge plagioclase from literature (Scott, 1980), shown for comparison in Fig. 4C. The compositional range displayed by the Site 1201 plagioclase is that expected for calc-alkaline basalts, basaltic-andesites and andesites (e.g., Ewart, 1982). The most extreme plagioclase composition, An_{95}, is likely that of a xenocryst out of equilibrium with the host rock, which is an evolved basalt (sample 195 1201D 15R-2, 61-65 cm; Table 4). Similar extremely An-rich plagioclase xenocrysts were found by Hawkins and Castillo (1998) in rocks from the Belau islands.

Alteration affected the rims of several plagioclase crystals, so that the analytical data presented above have been acquired mostly on crystal cores. When core-rim pairs were measurable, both normal and reverse chemical zoning has been found. One case of strong reverse zoning, from An_{69} in the core to An_{80} at the rim, has been detected in a crystal from a volcanic clast (sample 195 1201D 10R-4, 63-66 cm).

The plagioclase of Site 1201 basement basalts shows a more restricted compositional range (Fig. 4D), mostly from bytownite to labradorite (An_{77} to An_{55}), with only one andesine (An_{43}; D'Antonio and Kristensen, 2005a). The less calcic plagioclase rims detected in the basement rocks have been described for crystals whose cores, presumably richer in anorthite, were completely altered to secondary clay minerals, zeolites and/or calcite.

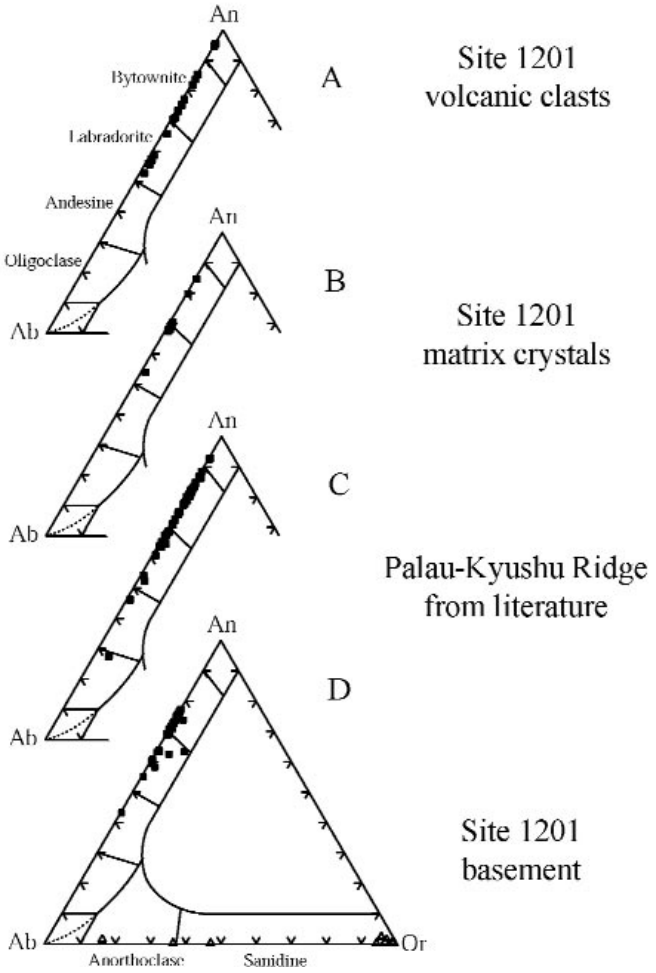

Fig. 4 - Ternary classification diagram Ab-An-Or for feldspars, showing the chemical variability of plagioclase of A) Site 1201 volcanic clasts (this work), B) Site 1201 matrix single crystals (this work), C) Palau-Kyushu Ridge (data from DSDP Leg 59, Sites 448, 448A and 451; Scott, 1980) and D) Site 1201 basement basalts (D'Antonio and Kristensen, 2005a). For the latter, the chemical variability of secondary alkali-feldspar is also shown. Ab- albite; An- anorthite; Or- orthoclase.

GEOTHERMOBAROMETRY

Geothermobarometric estimates for Site 1201 volcanic clasts can be made using both clinopyroxene-orthopyroxene, and plagioclase-liquid equilibria. For temperature calculations employing coexisting clinopyroxene and orthopyroxene pairs, we used the QUILF software, version 6.42, of Andersen et al. (1993). This provided estimates of 1,155 ± 56°C for the most primitive compositions found in volcanic clasts (Cpx: X_{En} = 0.451, X_{Wo} = 0.350; Opx: X_{En} = 0.687, X_{Wo} = 0.045), and 1,142 ± 12°C for those found in single crystals within the matrix (Cpx: X_{En} = 0.486, X_{Wo} = 0.369; Opx: X_{En} = 0.721, X_{Wo} = 0.043). Temperature estimates for the evolved pyroxene compositions gave values of 981 ± 17 °C for volcanic clasts (Cpx: X_{En} = 0.447, X_{Wo} = 0.322; Opx: X_{En} = 0.612, X_{Wo} = 0.029), and 989 ± 22°C for single crystals in the matrix (Cpx: X_{En} = 0.438, X_{Wo} = 0.349; Opx: X_{En} = 0.601, X_{Wo} = 0.031), respectively. The quite low uncertainties given by the calculations are good indication that the Cpx-Opx pairs selected for temperature estimates were in equilibrium. Independent temperature calculations have been carried out for two volcanic clasts (Savov et al., 2006) by using the plagioclase-liquid geothermometer, as recently refined by Putirka (2005) to provide also pressure estimates. The temperature and pressure estimated for the equilibrium between the basalt 195-1201D 5R-4, 136-138 cm and a plagioclase with An_{75} are 1477 ± 23 K (≅ 1204°C) and 6.3 ± 1.8 kbar, respectively; the estimates for the equilibrium between the andesite 195-1201D 10R-4, 63-65 cm and a plagioclase with An_{66} (Table 3) are 1345 ± 23 K (≅ 1072°C) and 2.9 ± 1.8 kbar, respectively.

The temperature values estimated with the two geothermometers are similar, considering the uncertainties. The overall temperature range, 1,160-980°C, agrees well with the basalt-andesite compositional spectrum shown by the analyzed PKR volcanic clasts; furthermore, the pressure estimates, even with their uncertainty (see discussion in Putirka, 2005), suggest a rough decreasing depth of crystallization for magmas varying in composition from basalt to andesite. A similar temperature range of 1,130-970°C was determined by Ishii (1980) using pyroxene geothermometry on DSDP Leg 59 basaltic to andesitic samples from Palau-Kyushu and West Mariana Ridges.

Estimates of temperature and pressure for Site 1201 basement basalt were carried out by D'Antonio and Kristensen (2005a). They estimated a temperature of 1,171°C for the equilibrium between the basalt 195-1201D 55R-1, 103-106 cm and the An-richest plagioclase microlite analyzed in that rock (An_{77}), using the plagioclase-liquid geothermometer of

Table 4 - XRF analyses and Sr-Nd isotopes of Site 1201 polymict tuffs

Sample	2R-1, 141-143	2R-2, 82-84	5R-4, 64-68	5R-4, 112-115	5R-5, 66-70	9R-1, 34-36	10R-4, 4-8	13R-6, 107-111	15R-2, 61-65	18R-3, 143-147	20R-1, 22-25	JB-1a
Classification	B	B	Hi-Mg ThB	B	B	B	B	B	B	B	A	B
SiO_2	54.39	55.53	53.33	49.01	55.51	54.65	54.77	55.15	56.04	56.13	55.72	53.25
TiO_2	0.63	0.65	0.53	0.51	0.58	0.70	0.63	0.66	0.64	0.61	0.68	1.33
Al_2O_3	17.06	17.69	16.84	17.89	18.38	18.13	18.36	17.86	17.49	17.89	16.74	14.92
Fe_2O_3tot	9.19	8.73	8.91	8.98	7.68	8.53	8.41	8.29	8.99	8.26	8.65	9.22
MnO	0.14	0.14	0.17	0.17	0.14	0.15	0.14	0.15	0.17	0.15	0.15	0.15
MgO	5.60	5.32	8.45	7.06	5.95	5.20	5.53	5.21	5.78	4.51	4.58	7.98
CaO	8.25	8.20	4.86	10.36	5.74	8.44	7.20	7.41	7.39	6.25	6.41	9.50
Na_2O	3.04	3.10	3.85	3.34	3.84	2.93	3.58	3.34	2.84	5.19	5.35	2.81
K_2O	0.86	0.85	1.84	0.97	1.58	0.60	1.25	1.26	0.88	1.19	1.09	1.45
P_2O_5	0.09	0.08	0.32	1.98	0.08	0.10	0.13	0.18	0.12	0.11	0.14	0.26
Sum	99.25	100.29	99.10	100.27	99.48	99.43	100.00	99.51	100.34	100.29	99.51	100.87
LOI	8.72	6.40	13.66	9.13	15.69	9.71	12.33	11.55	11.94	11.49	12.62	n.a.
$CaCO_3$	10.8	5.8	8.3	5.8	9.2	9.7	5.0	5.0	n.a.	n.a.	n.a.	n.a.
Mgv	57.8	57.8	68.1	63.9	63.5	57.8	59.7	58.6	59.1	55.1	54.3	66.1
Sc	18	16.1	21	12.7	20	17.0	19	18	16.5	20	21	22
V	222	243	228	235	255	256	239	241	242	224	260	217
Cr	60	68	60	29	65	54	39	58	44	32	44	420
Co	30	25	31	29	23	24	25	24	23	24	26	39
Ni	34	33	40	26	28	22	22	28	23	20	24	139
Cu	108	110	100	146	106	152	100	130	135	125	202	55
Zn	96	82	85	87	71	79	72	74	78	69	78	83
Rb	21	22	30	22	30	21	28	29	25	31	29	41
Sr	253	265	163	307	202	250	209	222	226	308	468	456
Y	14.7	15.2	30	88	8.4	13.4	15.4	17.0	19	17.2	19	25
Zr	74	78	58	48	62	80	74	87	84	80	91	144
Nb	2.5	1.7	3.0	2.1	3.4	2.0	3.0	1.8	3.5	3.3	3.5	27
Ba	80	98	111	71	80	103	137	120	142	175	205	507
La	43	10	39	54	15.5	25	21	16.5	40	34	26	43
Ce	6.5	16.3	29	59	5.1	40	25	13.0	22	21	26	72
Nd	20	5.6	22	26	1.6	13.6	18	10.1	10.5	5.2	8.0	19
Th	1.3	1.4	1.3	1.5	1.5	1.9	1.3	1.5	1.6	1.2	1.6	7
U	0.6	0.7	1.0	0.7	1.0	0.6	0.9	0.9	0.9	0.7	0.9	2
$(^{87}Sr/^{86}Sr)_{meas}$	0.703433	0.703452	0.703558	0.703435	n.a.	0.703396	0.703464	0.703418	0.703525	0.703740	n.a.	n.a.
2σ	0.000005	0.000005	0.000005	0.000006	-	0.000004	0.000005	0.000005	0.000005	0.000004	-	-
$(^{143}Nd/^{144}Nd)_{meas}$	0.513035	0.513016	n.a.	n.a.	n.a.	n.a.	0.513014	n.a.	n.a.	0.512968	n.a.	n.a.
2σ	0.000012	0.000010	-	-	-	-	0.000012	-	-	0.000005	-	-
$(^{143}Nd/^{144}Nd)_{35\ Ma}$	0.512999	0.512980	-	-	-	-	0.512978	-	-	0.512929	-	-

All sample labels are preceded by 195-1201D. Major oxides are reported as wt.%, trace elements as p.p.m. n.a. = not analyzed. Major oxide and trace element analyses were made by X-ray fluorescence spectrometry, whereas $CaCO_3$ was determined by volumetric calcimetry, at University of Padova. Typical analytical uncertainty is <0.5% for silica, <3% for all other major oxides, and <5% for trace elements. Key for classification (Jensen cation plot, Rickwood, 1989): High-Mg ThB = high-Mg tholeiite basalt; B = basalt; A = andesite; BA = basaltic andesite. Sr- and Nd-isotope analyses were made by thermal ionization mass spectrometry, at I.N.G.V.-Osservatorio Vesuviano, Napoli. All powdered samples were repeatedly leached with hot 6N HCl before chemical dissolution in pure HF-HCl-HNO_3 mixtures and ion-exchange chromatography to isolate Sr and Nd. $^{87}Sr/^{86}Sr$ and $^{143}Nd/^{144}Nd$ ratios were normalized to $^{86}Sr/^{88}Sr = 0.1194$ and $^{146}Nd/^{144}Nd = 0.7219$, respectively, for within-run isotopic fractionation. The mean measured value of $^{87}Sr/^{86}Sr$ for NIST SRM 987 was 0.710250 ± 0.000014 (2σ, N = 56) and that of $^{143}Nd/^{144}Nd$ for La Jolla was 0.511850 ± 0.000015 (2σ, N = 25) during the period of measurements. Sr blank was less than 1 ng, and thus negligible for the measured samples. Meas = measured. Nd isotope ratios at 35 Ma are calculated according to Faure (1986, and quoted references).

Kudo and Weill (1970) refined by Mathez (1973). A slightly higher temperature of 1304 ± 23 K (≅ 1,203°C), and a pressure of 4.99 ± 1.8 kbar can be calculated by applying the formulation of Putirka (2005) to the same plagioclase-rock pair. The latter T and P estimates agree well with those carried out by D'Antonio and Kristensen (2005a) using the geothermobarometer clinopyroxene-liquid (Putirka et al., 1996), which gave average temperatures of 1195°C (N = 46, st. dev = 22°C) and pressure of 4.7 kbar (N = 43; st. dev. = 1.9 kb). Both temperature and pressure estimates are in agreement with the primitive nature of the parent tholeiitic basalt magma of Site 1201 basement.

GEOCHEMISTRY

Bulk rock major oxide and trace element contents

In Table 4 new X-ray fluorescence (XRF) major and trace element data for 11 representative Site 1201 polymict tuffs (composites of several volcanic clasts plus matrix) are listed. The new geochemical data are plotted on classification and tectono-magmatic discrimination diagrams (Figs. 5-7). In these diagrams, comparisons can be made with: the data field for other PKR volcanic rocks (Armstrong and Nixon, 1980; Ishii, 1980; Mattey et al., 1980; Scott, 1980; Hawkins and Castillo, 1998; Pearce et al., 1999); three individual PKR volcanic clasts, and WPB basement basalts, from ODP Site 1201 (Salisbury, Shinohara, Richter, et al., 2002; Savov et al., 2006); WPB basement lavas from DSDP Sites 291 and 447 (Pearce et al., 2005). The three individual Site 1201 volcanic clasts studied by Savov et al. (2006) and the polymict tuffs of the present work will be hereafter referred to as Site 1201 PKR volcanics.

Considering the advanced alteration and/or low-T metamorphism experienced by the investigated volcanic rocks, classification diagrams based on mobile elements, such as the Total Alkali-Silica diagram (Le Bas et al., 1986) may be unreliable. The high degree of alteration is clearly evident considering the high loss on ignition (L.O.I.; 6.4 - 15.7 wt%) and $CaCO_3$ contents (5.0 - 10.8 wt%; Table 4), which confirm petrographic observations for presence of diffuse zeolites, clay minerals, iron oxyhydroxides, and calcite. The very high L.O.I. values of some samples are due to the fact that they are composites including both clasts and clay rich-matrix. Thus, in order to better classify the Site 1201 PKR volcanics, the Jensen cation plot, which is based on the poorly mobile elements Al, Fe, Ti and Mg (Rickwood, 1989; Fig. 5) has been adopted. On this diagram, the Site 1201 PKR volcanics fall in the field of calc-alkaline series and classify mostly as basalt, with a few andesites. It is interesting to note that they are compositionally distinct from literature data for the Palau-Kyushu Ridge. Furthermore, Site 1201 PKR volcanics show a limited overlap with WPB basement basalts, the latter having distinctly less aluminium. These compositional differences will be treated in the discussion section.

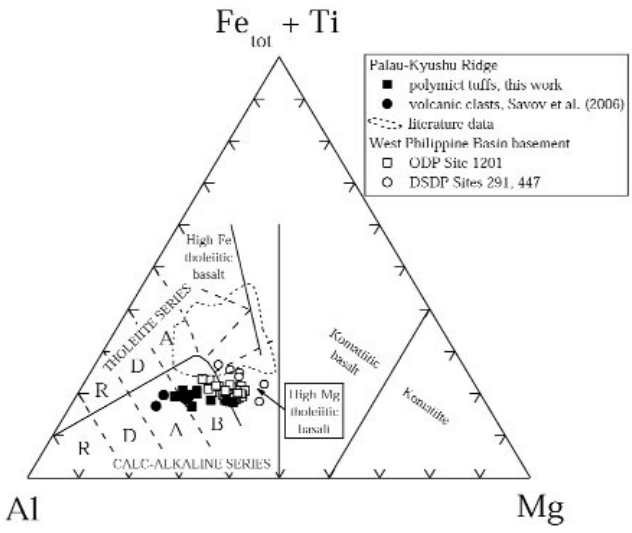

Fig. 5 - Jensen cation classification diagram (Rickwood, 1989) for Site 1201 PKR volcanics (data from Table 4 and from Savov et al., 2006). Literature data for PKR refer to both drilled (DSDP Leg 59, Sites 448, 448A and 451) and outcropping rocks on Palau, Guam and Saipan Islands (Armstrong and Nixon, 1980; Ishii, 1980; Mattey et al., 1980; Scott, 1980; Hawkins and Castillo, 1998; Pearce et al., 1999). West Philippine Basin basalts are from ODP Site 1201 (Salisbury, Shinohara, Richter, et al., 2002) and DSDP Sites 291 and 447 (Pearce et al., 2005).

The calc-alkaline affinity of Site 1201 PKR volcanics can be clearly seen in the Miyashiro's discrimination diagrams (Fig. 6), although one sample (Savov et al., 2006) falls in the tholeiitic field in the SiO_2 vs. FeO_{tot}/MgO plot. In that respect, the Site 1201 PKR volcanics differ from PKR literature data, most of which have either boninitic or low-K tholeiitic affinities (Armstrong and Nixon, 1980; Ishii, 1980; Mattey et al., 1980; Scott, 1980; Hawkins and Castillo, 1998; Pearce et al., 1999). It is interesting that the WPB basement basalts straddle the boundary between the tholeiitic and calc-alkaline fields on the two diagrams.

The high degree of alteration of the studied volcanic rocks prevents drawing meaningful variation diagrams, such as Harker's diagrams against a differentiation index. However, the available geochemical data allow us to make some comparison with other PKR and WPB samples on tectono-magmatic discrimination diagrams. In order to do that, only diagrams employing fluid-immobile major oxides and/or trace elements (e.g., Ti, V, Zr, Nb and Y) should be selected for such altered rocks. The Ti-V discrimination diagram (Shervais, 1982; Fig. 7) shows well the arc tholeiite affinity of both Site 1201 PKR volcanics and other PKR samples from the literature (Armstrong and Nixon, 1980). It is interesting that WPB basalts from ODP Site 1201 and DSDP Sites 291 and 447 fall partly in the field of MORB and back-arc basin basalts (BABB), and partly in that for arc tholeiites. Moreover, other WPB basalts, in particular those from DSDP Sites 292 and 294 (Pearce et al., 2005; Hickey-Vargas et al., in press), have a clear Ocean Island Basalt (OIB) affinity. Thus, immobile trace element data confirm and reinforce the difference between the Palau-Kyushu Ridge volcanics and the West Philippine Basin basalts.

Savov et al. (2006) have recently pointed out other trace element characteristics of both basement basalts (WPB) and some representative volcanic clasts recovered at Site 1201. As expected for back-arc basalts formed close to an active island arc, REE patterns of WPB basalts are LREE-depleted to flat. MORB-normalized spiderdiagrams are arc-like with variable degrees of LILE-enrichments, large negative Nb and Ta anomalies, and positive Sr and La anomalies. These patterns strongly resemble those of younger Mariana Trough back-arc basalts and modern low-K Mariana Arc volcanics (e.g., Arculus et al., 1995; Elliott et al., 1997). The PKR volcanic clasts show MORB-normalized patterns similar to those of modern Mariana Arc volcanics with calc-alkaline affinity, with high LILE abundances and deep negative Nb anomalies. The REE patterns are arc-like with

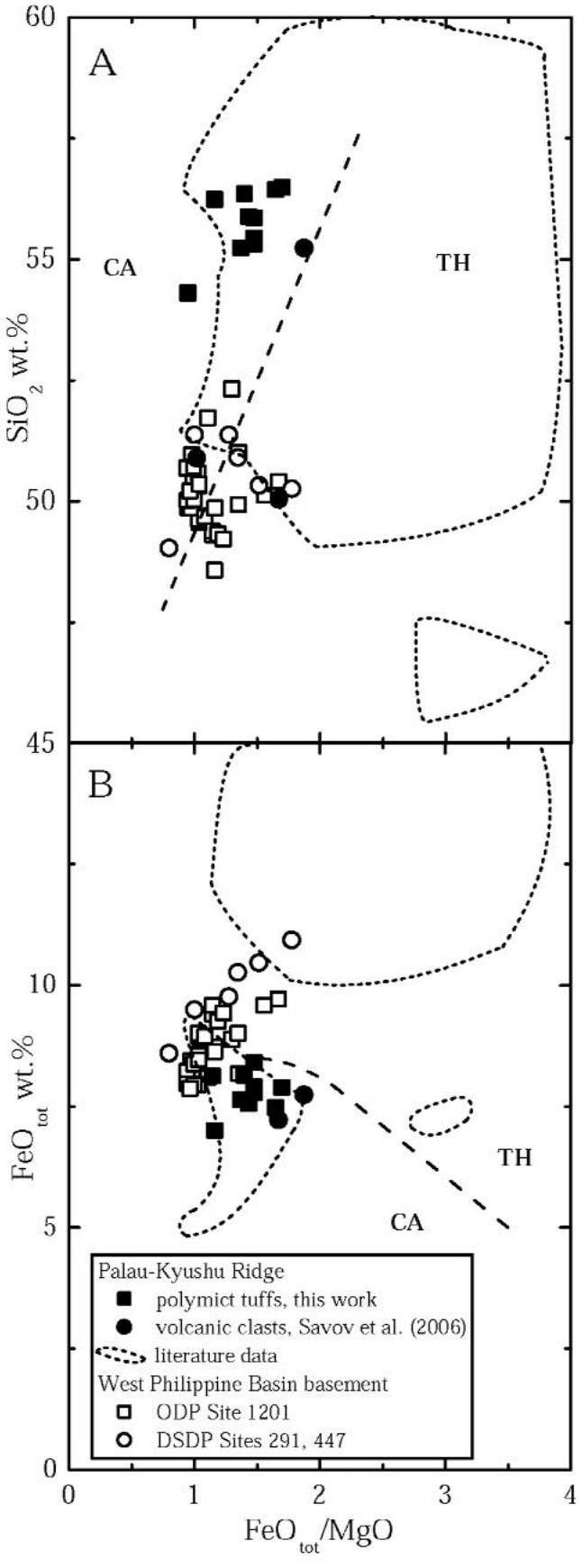

Fig. 6 - Diagrams for tectono-magmatic discrimination. A) SiO_2 and B) FeO_{tot} against FeO_{tot}/MgO (Miyashiro, 1974). TH, tholeiitic; CA, calc-alkaline. Literature data for PKR and WPB as in caption of Figure 5.

strong LREE enrichment. It is worthwhile to point out that modern Mariana Arc volcanics have strongly variable affinity, from sub-alkaline to shoshonitic lithological types (e.g., Peate and Pearce, 1998; Sun and Stern, 2001; Pearce et al., 1999; 2005).

Isotope geochemistry

New Sr- and Nd-isotope data for nine Site 1201 PKR polymict tuff samples are presented in Table 4. The Nd-isotope ratios are reported both as measured and age-corrected (to 35 Ma), whereas Sr-isotope ratios were not age-corrected. Since the powders have been long leached with hot 6N HCl to remove alteration, it is likely that the leaching procedure have significantly affected the original Rb and Sr content of the rocks. It is likely that the residue left after the leaching was made up only of plagioclase and clinopyroxene. These minerals do not contain appreciable amounts of Rb, whereas they are quite rich in Sr. Thus, their Rb/Sr ratio must be very low, and the Sr-isotope ratio measured on leached samples can be reasonably assumed as the initial.

Initial $^{87}Sr/^{86}Sr$ ratios range between 0.70340 and 0.70374; initial $^{143}Nd/^{144}Nd$ ratios vary between 0.51293 and 0.51300. Savov et al. (2006) report slightly more radiogenic initial $^{87}Sr/^{86}Sr$ ratios, in the range 0.70338-0.70432, with homogeneous initial $^{143}Nd/^{144}Nd$ ratios (0.51297-0.51298), for three Site 1201 volcanic clasts. Isotope data for the Palau-Kyushu Ridge in the literature are very scarce. The few published data are for rocks drilled by DSDP during Leg 59 at Sites 448 and 448A, and for Eocene formations cropping out at Palau, Saipan and Guam islands. These rocks have initial $^{87}Sr/^{86}Sr$ ratios in the range 0.70307-0.70355, and initial $^{143}Nd/^{144}Nd$ ratios in the range 0.51302-0.51306 (Armstrong and Nixon, 1980; Hickey-Vargas, 1991; Pearce et al., 1999). One sample with extremely high $^{87}Sr/^{86}Sr$ ratio of 0.706267, and $^{143}Nd/^{144}Nd$ ratio of 0.513048, reported by Pearce et al. (1999), is likely severely altered by seawater.

In the Sr-Nd covariation plot (Fig. 8A), comparisons can be made among Site 1201 PKR volcanics and WPB basement (Savov et al., 2006; this work), other WPB basement rocks (Hickey-Vargas, 1998b; Hickey-Vargas et al., in press) and the fields of Pacific and Indian Ocean MORBs, and the active Mariana Arc (Hickey-Vargas and Reagan, 1987; Elliott et al., 1997). The basement basalts and most PKR volcanics of Site 1201 fall within the field of Indian Ocean MORB, although the latter fall at distinctly lower initial $^{143}Nd/^{144}Nd$ values. Two volcanic clasts which are enriched in radiogenic Sr with respect to the other samples are shifted rightwards, falling outside the field of the active Mariana Arc. These samples were likely severely altered by seawater and the leaching procedure, carried out with dilute acid (0.1 N HCl) before dissolution and isotopic analysis (Savov et al., 2006), did not remove effectively all seawater-derived Sr. Apart from these two samples, all the Site 1201 PKR volcanics fall at the enriched end of Indian Ocean MORB field, and also plot within the field of active Mariana Arc. Other PKR volcanic rocks from the literature plot within this field too, but at distinctly higher initial $^{143}Nd/^{144}Nd$ values.

The isotopic similarity of Site 1201 basement basalts to Indian Ocean MORB, notwithstanding they have been emplaced in the Western Pacific Ocean, is a common characteristic of other West Philippine Basin basement basalts (Hickey-Vargas, 1991; Hickey-Vargas et al., 1995; Spadea

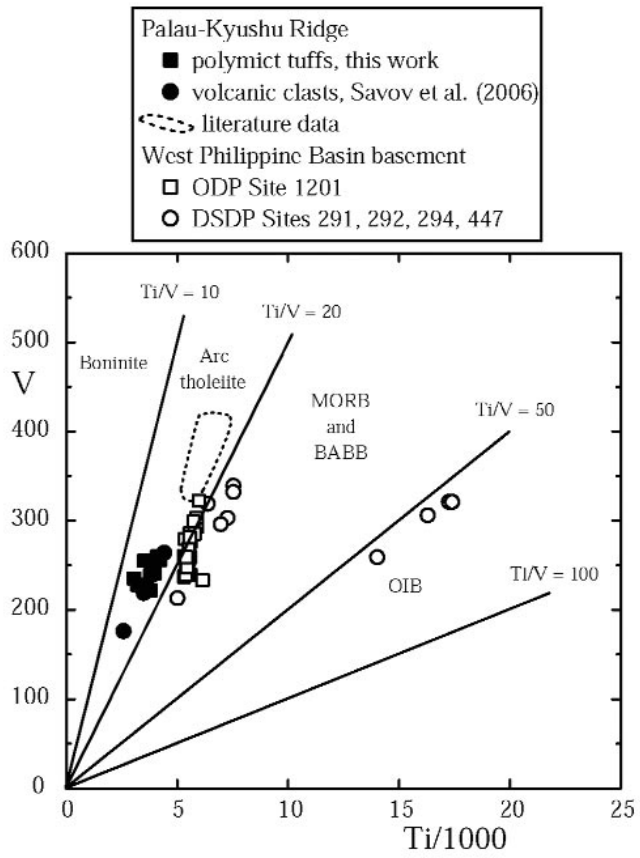

Fig. 7 - Tectono-magmatic discrimination diagram Ti-V (p.p.m.). MORB: mid-ocean ridge basalts; BABB: back-arc basin basalts; OIB: ocean island basalts (Shervais, 1982). Literature data for PKR and WPB as in caption of Fig. 5.

et al., 1996; Hickey-Vargas, 1998a; 1998b; Savov et al., 2006; Hickey-Vargas et al., in press). This isotopic feature is shared also by the Palau-Kyushu Ridge volcanics, as observed first by Pearce et al. (1999), and then by Savov et al. (2006) and confirmed by the new isotope dataset presented here (Table 4 and Fig. 8). For both the basement basalts and the volcanic clasts recovered at Site 1201, Savov et al. (2006) also found Pb- and Hf-isotopic evidence for an Indian Ocean MORB affinity. Indeed, most of the Site 1201 basement basalts and volcanic clasts have higher $^{208}Pb/^{204}Pb$ for a given $^{206}Pb/^{204}Pb$. Also, they have higher $^{176}Hf/^{177}Hf$ for a given $^{143}Nd/^{144}Nd$, compared with Pacific Ocean MORB, as is clearly visible on Fig. 8B. The Indian Ocean MORB Nd-Hf isotope signatures were recently described for WPB basalts from other locations (Pearce et al., 1999; Hickey-Vargas et al., in press).

DISCUSSION AND CONCLUSIONS

The rock sequence recovered at Site 1201 Hole D during Leg 195 has an inherent importance, as noted by Salisbury, Shinohara, Richter, et al. (2002), Salisbury et al. (2006) and Savov et al. (2006), and emphasized here. Indeed, these rocks provide a unique opportunity to investigate the geochemical and isotopic features of volcanic rocks from a now-extinct intra-oceanic volcanic arc, the Palau-Kyushu Ridge, and from the back-arc basin related to the activity of that same arc, i.e. the West Philippine Basin. Volcanic rocks belonging to the now submerged PKR crop out in very few locations (Palau, Saipan, Guam and Belau Islands; e.g., Hickey-Vargas and Reagan, 1987; Hawkins and Castillo, 1998; Pearce et al., 1999). Thus, Site 1201 volcanic clasts from turbidite deposits, generated when the arc was emerged, are of great importance to better characterize the history of the early IBM volcanic arc.

The mineral chemistry investigation carried out on pyroxene and plagioclase of Site 1201 volcanics has highlighted clinopyroxene of magnesium-rich augite composition, orthopyroxene of ferroan enstatite composition, along with bytownite-labradorite plagioclase, amphibole, olivine and opaque oxides (Tables 1-3; Figs. 3-4). This is a mineralogical association typical, though not exclusive, of calc-alkaline basalts and andesites (e.g., Ewart, 1982). The Site 1201

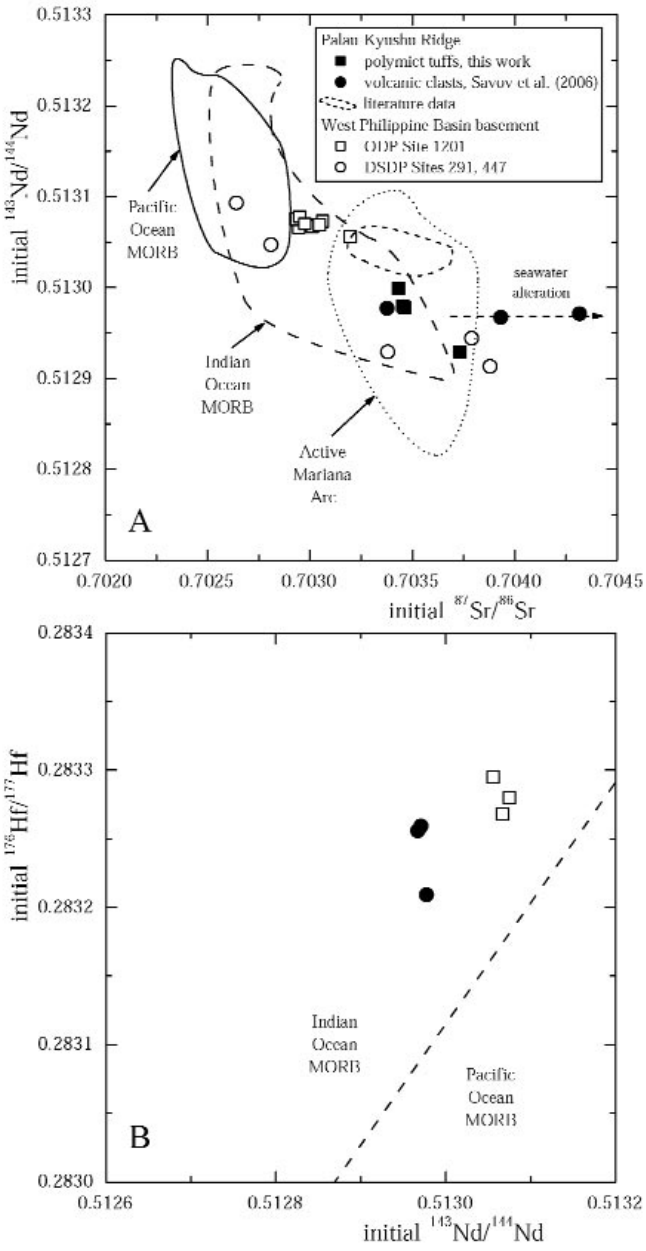

Fig. 8 - A) initial $^{87}Sr/^{86}Sr$ versus $^{143}Nd/^{144}Nd$ ratios and B) initial $^{143}Nd/^{144}Nd$ versus $^{176}Hf/^{177}Hf$ ratios for Site 1201 PKR volcanics (data from Table 4, and Savov et al., 2006). Fields of Pacific and Indian Ocean MORB are from Savov et al. (2006) and quoted references. Field of active Mariana Arc is from Hickey-Vargas and Reagan (1987). Literature data for PKR volcanics are from Hickey-Vargas (1991) and Pearce et al. (1999). Data for WPB basement are from Savov et al. (2006; ODP Site 1201), and Hickey-Vargas (1998b; DSDP Sites 447 and 291).

basement basalts to the contrary, are characterized only by Mg-rich augite, in addition to olivine, bytownite-labradorite plagioclase and opaque oxides, i.e. an association more typical of tholeiitic basalts (D'Antonio and Kristensen, 2005a).

The results of geothermobarometric estimates carried out on PKR volcanic clasts suggest that the magmas were evolving through fractional crystallization processes from basalt to andesite compositions, in a temperature range between ca. 1160 and 980°C, at a pressure decreasing from ca. 6.3 to 2.9 kbar. In agreement with the more primitive nature of their tholeiitic parent magma, the basement basalts drilled at Site 1201 appear to have equilibrated at slightly higher temperatures, ca. 1200°C, with respect to that of PKR volcanics, and at pressures of ca. 5 kbar, (D'Antonio and Kristensen, 2005a; this work).

One of the most interesting results of this investigation concerns the geochemical affinity of the studied Site 1201 PKR volcanics. When plotted on classification and tectono-magmatic discrimination diagrams using elements poorly sensitive to alteration (Figs. 5-7), the investigated Site 1201 PKR volcanics reveal well their calc-alkaline affinity. This is at variance with most of the other PKR samples available in the literature, which have either boninitic or low-K tholeiitic affinity (Armstrong and Nixon, 1980; Ishii, 1980; Mattey et al., 1980; Scott, 1980; Hawkins and Castillo, 1998; Pearce et al., 1999). The calc-alkaline nature of Site 1201 PKR volcanics is also confirmed by their pyroxene composition, as was pointed out earlier. The underlying Site 1201 basement basalts fall between the calc-alkaline and the tholeiitic fields. Particularly interesting is the position of these rocks when they are plotted on the Ti vs. V diagram, where they straddle the boundary between the field of tholeiites and that of back-arc basin basalts/mid-ocean ridge basalts (Fig. 7).

The initial Sr- and Nd-isotope ratios of all the Site 1201 volcanic rocks (Fig. 8; Savov et al., 2006; Hickey-Vargas et al., in press; this work) are similar to the most enriched Indian Ocean MORBs. Moreover, they fall within the field of the currently active Mariana Arc, suggesting similarity of source region characteristics and/or magmatic processes between the early arc, i.e. the Palau-Kyushu Ridge, and the current Izu-Bonin-Mariana arc-basin system. However, we pointed out that the Site 1201 PKR volcanics have initial $^{143}Nd/^{144}Nd$ values distinctly lower than those of other PKR volcanic rocks, for a similar range of initial $^{87}Sr/^{86}Sr$ values. The observation that the PKR volcanic rocks have mostly boninitic and low-K tholeiitic affinity, whereas the investigated Site 1201 PKR volcanics have calc-alkaline affinity, appears consistent with the difference in their initial $^{143}Nd/^{144}Nd$ ratio. The lower initial $^{143}Nd/^{144}Nd$ suggests that Site 1201 samples could represent magmas derived from an Indian Ocean MORB-like source region, modified by a higher amount of subduction-related components (aqueous fluids and clay-rich sediment or sediment melts; see Savov et al., 2006) compared to those inferred for the boninites and low-K tholeiites emplaced during earlier stages of arc development.

The nature of the subduction components added to the mantle source can be better highlighted by means of binary diagrams employing ratios of trace elements with similar incompatibilities, one subduction-mobile and one subduction-immobile, divided by a trace element that is incompatible and highly conservative in subduction systems (Pearce et al., 2005). Following the approach of Pearce et al. (2005), we constructed a Th/Y vs. Nb/Y diagram (Fig. 9). In this plot, all the West Philippine Basin basalts (ODP Site 1201 and DSDP Sites 291, 292, 294 and 447) define a MORB-OIB array which best represents the local mantle domain. Offsets in the Th/Y ratio from this mantle array are manifestation of subduction-related additions. Given the geochemical characteristics of Th (Elliott et al., 1997), the subduction input highlighted in Fig. 9 must represent addition of siliceous melts (Pearce et al., 2005 and quoted references). This diagram also provides quantification of the subduction input, and for Site 1201 PKR volcanics, the contribution is bracketed between 75 and over 90%, or essentially the same as the modern Mariana arc volcanics.

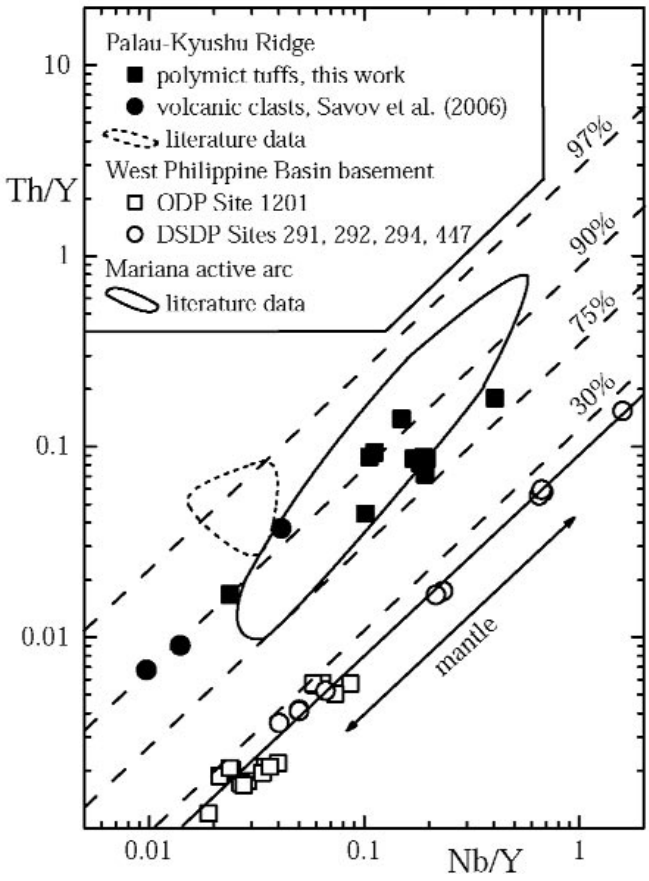

Fig. 9 - Th/Y vs. Nb/Y diagram for Site 1201 PKR volcanics (data from Table 4, and Savov et al., 2006). The contours provide the percentages of Th added to the mantle by subduction. Literature data for PKR and WPB as in caption of Fig. 5. Literature data for Mariana arc from Pearce et al., 2005 and quoted references.

The role of aqueous fluids cannot be investigated in the PKR volcanics due to the sensitivity to alteration of commonly used element tracers such as Ba, Sr and K. However, the Th enrichment with respect to Nb (as shown in Fig. 9) testifies to the significant role of siliceous melts, i.e. deep components, as contribution to the mantle from subduction, most possibly during the late stage PKR arc volcanism. Thus, the generation of the calc-alkaline volcanics investigated in this study could have occurred during an evolved stage of arc volcanism at Palau-Kyushu Ridge, perhaps shortly before the end of its activity, which may have occurred as late as 29 Ma (Scott and Kroenke, 1983). Indeed, according to the geological and geochronological reconstruction of the early IBM arc resulting by the study of terranes cropping out at Guam, Palau, Saipan and Belau islands (e.g., Hickey-Vargas and Reagan, 1987; Hawkins and Castillo, 1998; Pearce et al., 1999), volcanism began with

emplacement of boninitic rocks in the Middle Eocene, and later evolved into tholeiitic and finally calc-alkaline series rocks in Early-Middle Oligocene. The Site 1201 calc-alkaline volcanics belong to the uppermost ca. 250 meters (Cores 1R-18R) of a turbidite sequence dated Late Eocene - Middle Oligocene (Salisbury, Shinohara, Richter, et al., 2002). Thus, a Middle Oligocene age can be inferred for these rocks, in agreement with an evolved activity stage of the Palau-Kyushu Ridge. Further investigations on more volcanic clasts, particularly those occurring in deeper cores at Site 1201, will be necessary in order to clarify better the earlier evolution of the Palau-Kyushu Ridge arc volcanism.

ACKNOWLEDGMENTS

I. Arienzo, V. Di Renzo and F. Giordano are thanked for their help in Sr- and Nd-isotope measurements at I.N.G.V., Osservatorio Vesuviano. Assistance by D. Pasqual during XRF analyses at University of Padova is appreciated. Tom Beasley is thanked for assistance during the EMP sessions at Florida Center for Analytical Electron Microscopy, Florida International University, Miami. Jeff Ryan is thanked for valuable advice on an earlier version of the manuscript. Careful revision by J. Pearce and S. Tonarini, and the editorial activity of A. Montanini greatly improved the article and are much appreciated. This work was financially supported by Ricerca Dipartimentale 2005 and 2006 funds to M.D.

REFERENCES

Andersen D.J., Lindsley D.H. and Davidson P.M., 1993. QUILF: a PASCAL program to assess equilibria among Fe-Mg-Ti oxides, pyroxenes, olivine and quartz. Comp. Geosci., 19: 1333-1350.

Arculus R.J., Gill J.B., Cambray H., Chen W. and Stern R.J., 1995. Geochemical evolution of arc systems in the western Pacific: the ash and turbidite record recovered by drilling. In: B. Taylor and J. Natland (Eds.), Active margins and marginal basins of the Western Pacific, Am. Geophys. Un., Geophys. Monogr. Ser., 88: 45-65.

Armstrong R.L. and Nixon G.T., 1980. Chemical and Sr-isotopic composition of igneous rocks from Deep Sea Drilling Project Legs 59 and 60. In: L. Kroenke, R. Scott et al. (Eds.), Init. Repts. D.S.D.P., 59: 719-727.

Cosca M.A., Arculus R.J., Pearce J.A. and Mitchell J.G., 1998. $^{40}Ar/^{39}Ar$ and K/Ar age constraints for the inception and early evolution of the Izu-Bonin-Mariana arc system. Island Arc, 7: 579-595.

D'Antonio M. and Kristensen M.B., 2005a. Data report: electron microprobe investigation of primary minerals of basalts from the West Philippine Sea Basin (Ocean Drilling Program Leg 195, Site 1201). In: M. Shinohara, M.H. Salisbury and C. Richter (Eds.), Proc. ODP, Sci. Res., 195: 1-24 [Online]. Available from World Wide Web: http://www-odp.tamu.edu/publications/195_SR/VOLUME/CHAPTERS/108.PDF.

D'Antonio M. and Kristensen M.B., 2005b. Hydrothermal alteration of oceanic crust in the West Philippine Sea Basin (Ocean Drilling Program Leg 195, Site 1201): inferences from a mineral chemistry investigation. Mineral. Petrol., 83 (1-2): 87-112.

Deschamps A. and Lallemand S., 2002. The West Philippine Basin: an Eocene to Early Oligocene back arc basin opened between two opposed subduction zones. J. Geophys. Res., 107(B12), 2322, doi: 10.1029/2001JB001706, 2002.

Deschamps A., Lallemand S. and Dominguez S., 1999. The last spreading episode of the West Philippine Basin revisited. Geophys. Res. Lett., 26: 2073-2076.

Deschamps A., Okino K. and Fujioka K., 2002. Late amagmatic extension along the central and eastern segments of the West Philippine Basin fossil spreading axis. Earth Planet. Sci. Lett., 203: 277-293.

Dungan M.A., Rhodes J.M., Long P.E., Blanchard D.P., Brannon J.C. and Rodgers K.V., 1978. The petrology and geochemistry of basalts from Site 396, Legs 45 and 46 of the Deep Sea Drilling Project. In: L. Dmitriev, J. Heirtzler, et al., Init. Repts. D.S.D.P., 46: 89-114.

Elliott T., Plank T., Zindler A., White W.M. and Bourdon B., 1997. Element transport from subducted slab to juvenile crust at the Mariana Arc. J. Geophys. Res., 102: 14,991-15,019.

Ewart A., 1982. The mineralogy and petrology of Tertiary-Recent orogenic volcanic rocks, with special reference to the andesitic-basaltic compositional range. In: R.S. Thorpe (Ed.), Andesites: orogenic andesites and related rocks. John Wiley & Sons, Chichester, p. 25-98.

Faure G., 1986. Principles of isotope geology. Second edition, John Wiley & Sons, New York, 589 pp.

Fujioka K., Okino K., Kanamatsu T., Ohara Y., Ishizuka O., Haraguchi S. and Ishii T., 1999. Enigmatic extinct spreading center in the West Philippine backarc basin unveiled. Geology, 27: 1135-1138.

Hall R., 2002. Cenozoic geological and plate tectonic evolution of SE Asia and the SW Pacific: computer-based reconstructions, model and animations. J. As. Earth Sci., 20: 353-431.

Hall R., Ali J.R., Anderson C.D. and Baker S.J., 1995. Origin and motion history of the Philippine Sea Plate. Tectonophys., 251: 229-250.

Hawkins J.W. and Castillo P.R., 1998. Early history of the Izu-Bonin-Mariana arc system: Evidence from Belau and the Palau Trench. Island Arc, 7: 559-578.

Hickey-Vargas R., 1991. Isotope characteristics of submarine lavas from the Philippine Sea: implications for the origin of arc and basin magmas of the Philippine tectonic plate. Earth Planet. Sci. Lett., 107: 290-304.

Hickey-Vargas R., 1998a. Geochemical characteristics of ocean island basalts from the West Philippine basin: Implications for the sources of Southeast Asian plate margin and intraplate basalts. In: M. Flower, S.-L. Chung, C.H. Lo and T.-Y. Lee (Eds.), Mantle dynamics and plate interactions in East Asia. Am. Geophys. Un., Geodyn. Ser. Monogr., 27: 365-384.

Hickey-Vargas R., 1998b. Origin of the Indian Ocean-type isotopic signature in basalts from the West Philippine Sea plate spreading centers: An assessment of local versus large scale processes. J. Geophys. Res., 103: 20,963-20,979.

Hickey-Vargas R., Hergt J.M. and Spadea P., 1995. The Indian Ocean-type isotopic signature in West Pacific marginal basins: origin and significance. In: B. Taylor and J. Natland (Eds.), Active margins and marginal basins of the Western Pacific. Am. Geophys. Un., Geophys. Monogr. Ser., 88: 175-197.

Hickey-Vargas R. and Reagan M.K., 1987. Temporal variation of isotope and rare earth element abundances in volcanic rocks from Guam: implications for the evolution of the Mariana Arc. Contrib. Mineral. Petrol., 97: 497-508.

Hickey-Vargas R., Savov I.P., Bizimis M., Okino K., Fujioka K. and Ishii T. Origin of diverse geochemical signatures in igneous rocks from the West Philippine Basin: Implications for tectonic models. Am. Geophys. Un. Monogr., in press.

Hilde T.W.C. and Lee C.-S., 1984. Origin and evolution of the West Philippine Basin: a new interpretation. Tectonophysics, 102: 85-104.

Hodges F.N. and Papike J.J., 1977. Petrology of basalts, gabbros, and peridotites from DSDP Leg 37. In: F. Aumento, W.G. Melson, et al., Init. Repts. D.S.D.P., 37: 711-719.

Hussong D. and Uyeda S., 1981. Tectonic processes and the history of the Mariana arc: a synthesis of the results of Deep Sea Drilling Project Leg 60. In: M. Lee and R. Powell (Eds.), Init. Repts. D.S.D.P., 60: 909-929.

Ishii T., 1980. Pyroxene geothermometry of basalts and an andesite from the Palau-Kyushu and West-Mariana Ridges, Deep

Sea Drilling Project Leg 59. In: L. Kroenke, R. Scott et al. (Eds.), Init. Repts. DSDP, 59: 693-718.

Kudo A.M. and Weill D.F., 1970. An igneous plagioclase thermometer. Contrib. Mineral. Petrol., 25: 52-65.

Le Bas M.J., Le Maitre R.W., Streckeisen A. and Zanettin B., 1986. A chemical classification of volcanic rocks based on the total alkali-silica diagram. J. Petrol., 27: 745-750.

Mathez E.A., 1973. Refinement of the Kudo-Weill plagioclase thermometer and its application to basaltic rocks. Contrib. Mineral. Petrol., 41: 61-72.

Mattey D.P., Marsh N.G. and Tarney J., 1980. The geochemistry, mineralogy, and petrology of basalts from the West Philippine and Parece-Vela basins and from the Palau-Kyushu and West Mariana ridges, Deep Sea Drilling Project Leg 59. In: L. Kroenke, R. Scott et al. (Eds.), Init. Repts. D.S.D.P., 59: 753-800.

Mevel C., Ohnenstetter D. and Ohnenstetter M., 1978. Mineralogy and petrography of Leg 46 basalts. In: L. Dmitriev, J. Heirtzler, et al., Init. Repts. D.S.D.P., 46: 151-164.

Miyashiro A., 1974. Volcanic rock series in island arcs and active continental margins. Am. J. Sci., 274: 321-355.

Okino K., Ohara Y., Kasuga S. and Kato Y., 1999. The Philippine Sea: new survey results reveal the structure and the history of the marginal basins. Geophy. Res. Lett., 26: 2287-2289.

Pearce J.A., Kempton P.D., Nowell G.M and Noble S.R., 1999. Hf-Nd element and isotope perspective on the nature and providence of mantle and subduction components in Western Pacific arc-basin systems. J. Petrol., 40: 1579-1611.

Pearce J.A., Stern R.J., Bloomer S.H. and Fryer P., 2005. Geochemical mapping of the Mariana arc-basin system: implications for the nature and distribution of subduction components. Geochem. Geophys. Geosyst. 6, Q07006, doi: 10.1029/2004GC000895.

Peate D.W. and Pearce J.A., 1998. Causes of spatial compositional variations in Mariana arc lavas: trace element evidence. Island Arc, 7: 479-495.

Putirka K.D., 2005. Igneous thermometers and barometers based on plagioclase + liquid equilibria: Tests of some existing models and new calibrations. Am. Mineral., 90: 336-346.

Putirka K., Johnson M., Kinzler R., Longhi J. and Walker D., 1996. Thermobarometry of mafic igneous rocks based on clinopyroxene-liquid equilibria, 0-30 kbar. Contrib. Mineral. Petrol., 123: 92-108.

Rickwood P.C., 1989. Boundary lines within petrologic diagrams which use oxides of major and minor elements. Lithos, 22: 247-263.

Rock N.M.S., 1990. The International Mineralogical Association (IMA/CNMMN) pyroxene nomenclature scheme: computerization and its consequences. Mineral. Petrol., 43: 99-119.

Salisbury M.H., Shinohara M. and Richter C., et al., 2002. Proc. ODP, Init. Repts., 195, [Online]. Available from World Wide Web: http://www-odp.tamu.edu/publications/195_IR/195ir.htm.

Salisbury M.H., Shinohara M., Suetsugu D., Arisaka M., Diekmann B., Januszczak N. and Savov I.P., 2006. Leg 195 synthesis: Site 1201-a geological and geophysical section in the West Philippine Basin from the 660-km discontinuity to the mudline. In: M. Shinohara, M.H. Salisbury and C. Richter (Eds.), Proc. O.D.P., Sci. Res., 195: 1-27 [Online]. Available from World Wide Web: http://www-odp.tamu.edu/publications/195_SR/VOLUME/CHAPTERS/113.PDF.

Savov I.P., Hickey-Vargas R., D'Antonio M., Ryan J.G. and Spadea P., 2006. Petrology and geochemistry of West Philippine Basin basalts and early Palau-Kyushu arc volcanic clasts from ODP Leg 195, Site 1201D: implications for the early history of the Izu-Bonin-Mariana arc. J. Petrol., 47 (2): 277-299.

Scott R.B., 1980. Petrology and geochemistry of arc tholeiites on the Palau-Kyushu Ridge, Site 448, Deep Sea Drilling Project Leg 59. In: L. Kroenke, R. Scott et al. (Eds.), Init. Repts. D.S.D.P., 59: 681-692.

Scott R. and Kroenke L., 1983. Evolution of back arc spreading and arc volcanism in the Philippine Sea: Interpretation of Leg 59 DSDP results. In: D. Hayes (Ed.), The tectonic and geologic evolution of Southeast Asian Seas and Islands, Am. Geophys. Un., Geophys. Monogr., 23: 283-291.

Shervais J.W., 1982. Ti-V plots and the petrogenesis of modern and ophiolitic lavas. Earth Planet. Sci. Lett., 59: 101-118.

Spadea P., D'Antonio M. and Thirlwall M.F., 1996. Source characteristics of the basement rocks from the Sulu and Celebes Basins (Western Pacific): chemical and isotopic evidence. Contrib. Mineral. Petrol., 123: 159-176.

Stern R. J., Fouch M. J. and Klemperer S., 2004. An overview of the Izu-Bonin-Mariana subduction factory, In: Inside the subduction factory, J. Eiler (Ed.), Am. Geophys. Un. Monogr., 138: 175-223.

Sun C.H. and Stern R.J., 2001. Genesis of Mariana shoshonites: contribution of the subduction component. J. Geophys. Res., 106: 589-608.

Wood D.A., Varet J., Bougault H., et al., 1979. The petrology, geochemistry and mineralogy of North Atlantic basalts: A discussion based on IPOD Leg 49. In: B.P. Luyendyk, J.R. Cann, et al., Init. Repts. D.S.D.P., 49: 597-655.

Yavuz F., 2001. PYROX: a computer program for the IMA pyroxene classification and calculation scheme. Comp. Geosci., 27: 97-107.

Received, March 10, 2006
Accepted, November 11, 2006